# Full-Cell Quinone/Hydroquinone Supercapacitors based on partially reduced Graphite Oxide and Lignin/PEDOT electrodes

Adriana M. Navarro-Suárez,[a] Nerea Casado,[b] Javier Carretero-González,*[a,‡] David Mecerreyes,[b] and Teófilo Rojo*[a,c]

Lignin (Lig) and Lig/PEDOT characterization

Figure S1a shows the Fourier Transform Infrared (FTIR) Spectra of Lignin (Lig), Lig/PEDOT and PEDOT. All the Lig/PEDOT polymers exhibit vibration bands related to lignin and PEDOT structures and the intensity of the bands depend on the composition of the polymer. Lignin FTIR spectrum shows peaks at 1600, 1510 cm^{-1} (vibrations of aromatic ring), 1460, 1428 cm^{-1} (aromatic ring vibrations combined with methyl and methylene C-H deformations), 1212 cm^{-1} (C-C and C-O stretching vibrations) and 1040 cm^{-1} (C-O-C stretching vibrations). Conversely, PEDOT shows peaks at 1200, 1090, 1060 cm^{-1} (C-O-C stretching of ethylenedioxy group), 980, 840 cm^{-1} (C-S stretching) and 685 cm^{-1}.[1] The intensity of the peak at 1600 cm^{-1} attributed to the C=C stretching of the aromatic ring in lignin, is the nethermost in the Lig/PEDOT 20/80. On the contrary, the broad C-S stretching peak at 840 cm^{-1}, typical of PEDOT, has the lowest intensity in the Lig/PEDOT 60/40.
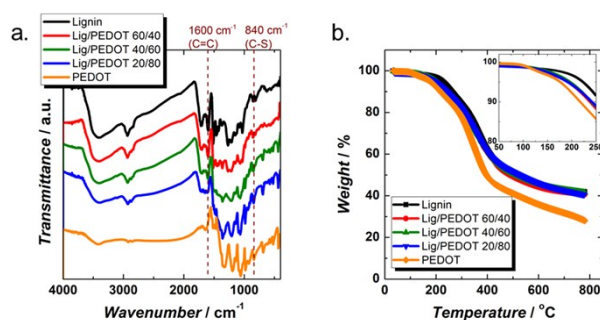
Figure S1. FTIR spectra (a) and TGA under nitrogen (b) of Lignin (Lig), PEDOT, Lig/PEDOT 40/60, Lig/PEDOT 60/40, and Lig/PEDOT 20/80.

The thermal stability of the polymers is investigated through thermo-gravimetric analysis (TGA). The Lig/PEDOT polymers show high thermal stability as shown in Figure S1b. All the Lig/PEDOT polymers are stable up to 190 ºC. Then, a continuous degradation occurs, corresponding to the elimination of absorbed water, and then a major decomposition in the region between 300 ºC and 450 ºC is observed, which is attributed to the decomposition of the PEDOT main chains.[2] Finally, at 800 °C, Lig/PEDOT polymers exhibit residual traces of 41 % of the total mass.

Partially reduced Graphite Oxide (prGrO) characterization

In order to determine the chemical structure of the partially reduced Graphite Oxide (prGrO), the material is analyzed by X-ray Photoelectron Spectra (XPS) (Figure S2) and Fourier Transform Infrared (FTIR) (Figure S3). Graphite Oxide (GrO) is also shown for comparison. The carbon and oxygen content present in the surface of prGrO is quantified by XPS. The shift in the XPS bands (Figure S2 a and b) of the GrO towards higher binding energies reflects a significant surface charging effect due to the electrically insulating nature of GrO. The C 1s spectrum of GrO in the top of Figure 2a has two main peaks at 285.5 eV and 287.3 eV that can be fit to peaks at 284.5, 285.5, 286.5, 287.7 and 288.7 eV and thus assigned to C=C, C-C, C-O, C-O-C and C=O, and C(O)OH respectively. Upon heating under argon flow, the C 1s spectrum exhibits a transformation from a double peak at room temperature to a single peak (~284.6 eV) at 160 °C, being indicative of a trend to restore the sp^2 bonding graphene character. This affirmation can be confirmed by the increase on the peak at 284.5 eV, related to C=C bonds, from 10.5 % to 67.3 % and the decrease of the peaks related to carbon directly attached to an oxygen atom. A clear shift of peak-maxima back to lower binding energy (BE) with increasing temperature signifies the transformation of electrically

[a]   Dr. A.M., Navarro-Suárez, Dr. Javier Carretero-González and Prof. T. Rojo
        CIC energiGUNE
        Albert Einstein 48, 01510 Miñano, Alava, Spain
[b]   N., Casado and Dr. D. Mecerreyes
        POLYMAT
        University of the Basque Country UPV/EHU
        Joxe Mari Korta Centre, Avda. Tolosa 72, 20018, Donostia-San Sebastian, Spain.
[c]   Prof. T. Rojo
        Inorganic Chemistry Department
        University of the Basque Country
        P.O. Box 644, 48080 Bilbao, Spain
        *E-mail: trojo@cicenergigune.com

[‡]   Current Address: Dr. J. Carretero-González
        Institute of Polymer Science and Technology, CSIC
        Juan de la Cierva 3, 28006, Madrid, Spain
   *E-mail: jabenzo@hotmail.com

insulated GO to the conducting nature of graphite. Comparing the C/O atomic ratio of GrO with prGrO, there is an increase in C-content and an associated decrease of the O groups, from 1.5 to 2.5.
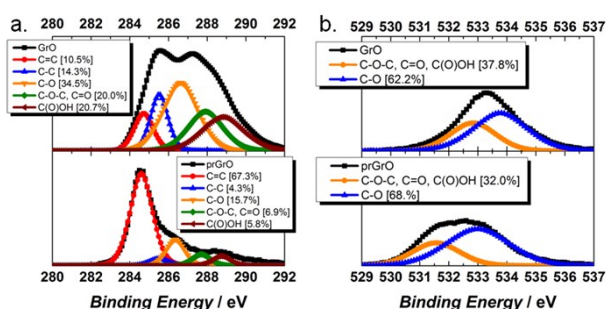
Figure S2. C 1s (a) and O 1s (b) survey by X-ray photoelectron spectroscopy of the Graphite oxide and the partially reduced Graphite oxide

Information provided by analysis of the O 1s spectra (Figure S2b) can complement the information provided by analysis of C 1s spectra, because the O 1s photoelectron kinetic energies are lower than those of the C 1s, the O 1s sampling depth is smaller, and therefore the O 1s spectra are slightly more surface specific. The peak corresponding to the C-O bonds increases from 62.2 % to 68.0 % during the thermal reduction, this could be explained by the formation of phenol (or aromatic diol) groups during deoxygenation because of the close proximity of C-OC and C-OH on the basal plane.

The changes in the functional groups from GrO to prGrO are followed with Fourier transform IR spectroscopy. This analysis is performed in a Hyperion 1000 FT-IR spectrometer, using about 5% of the GrO and prGrO grinded with KBr. Five main absorption bands are identified in the FTIR spectra (Figure S2), centered at 3400 cm^{-1} (O-H stretching vibrations), 1714 cm^{-1} (C=O stretching vibrations), 1620 cm^{-1} (skeletal vibrations from unoxidized graphitic domains), 1230 cm^{-1} (C-OH stretching vibrations) and 1160 cm^{-1} (C-O stretching vibrations).[3]
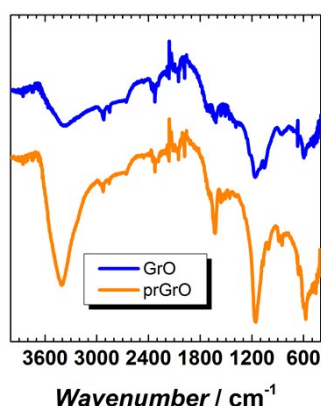
Figure S3. Fourier Transform Infrared of Graphite Oxide (GO) and partially reduced Graphite Oxide (prGrO)

Capacitive contributions to the current in Lignin

Given the electronically insulating character of lignin, a composite made out of lignin and Carbon Nanotubes (CNT) is physically mixed in a proportion 80:20 and its electrochemical properties are measured with the CME.

In Figure S4, Lignin-CNT presents a narrow peak around 0.52 V and its potential window is constricted between 0 and 0.9 V vs Ag/AgCl. When analyzing the capacitive contributions to the current, a small peak appears at 0.52 V, indicating that this peak is caused by both capacitive and diffusion-controlled processes. This peak might correspond to the redox process of the quinone groups present in the lignin,[4] and is present in both curves as result of the reaction occurring in both the surface of the material (pseudocapacitive process) and the bulk electrode. The remaining capacitive contribution might be caused by intercalation pseudo-capacitance and double-layer effect. The total capacitive contribution to the current is of 42 % at 100 mV s^{-1}.
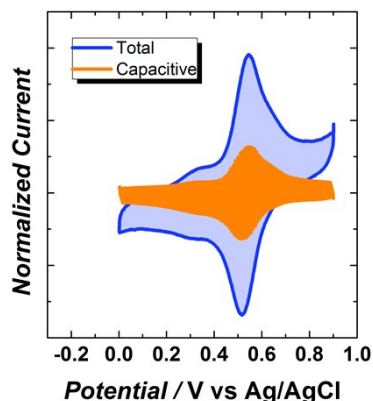
Figure S4. Total (blue area) and capacitive contributions (orange area) to charge storage in 0.1M $HClO_4$ of lignin.

Electrochemical properties of Lig/PEDOT in a three-electrode configuration

Figure S5 shows the rate capability of the different Lig/PEDOT proportions. The difference in capacitance between the different Lig/PEDOT ratios observed in in Figure S4a might be explained by the different Lig/PEDOT ratios in the electrode material. For instance, in Lig/PEDOT 20/80 the percentage of lignin is low then the redox reaction between quinone/hydroquinone is diminished while in Lig/PEDOT 60/40, the percentage of PEDOT might be too low, making it difficult for the electrons to transfer to the lignin blocks. The highest capacitance value, 97 F g^{-1}, is achieved by Lig/PEDOT 40/60.

Figure S5b relates the capacitance retention with the current density of different Lig/PEDOT polymers. The increment of lignin proportion on the polymer increases the capacitance retention with the current density. This might seem counterintuitive, as the PEDOT should be increasing the conductivity of the material. However, as explained by Ajjan *et al.*, Lignin acts in the polymer as both dopant and dispersing agent,[1] therefore its decrease might cause a charge unbalance that reflects on a more difficult charge transport, hence a drop in the capacitance with the current density.
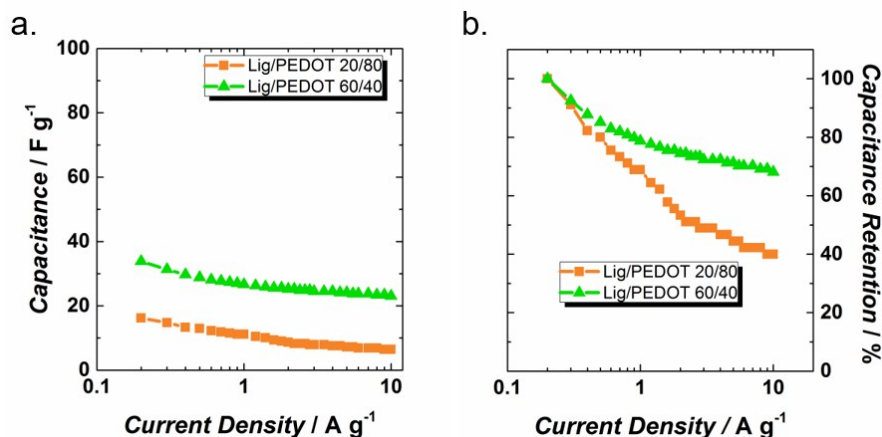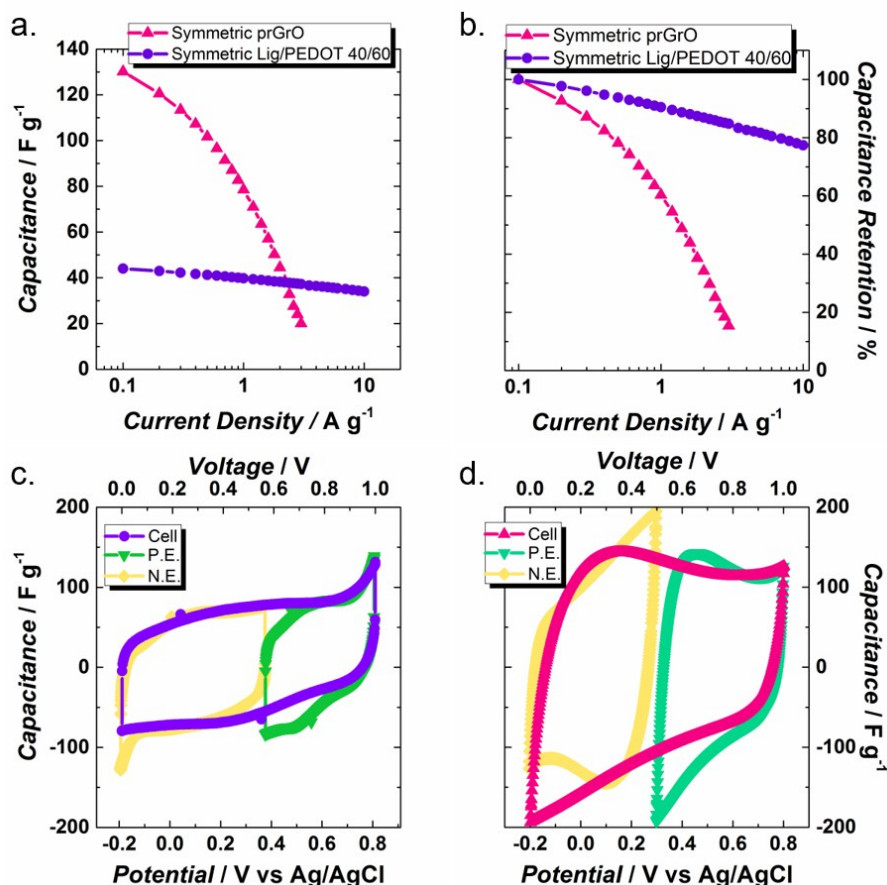

Figure S5. Rate capability (a) and capacitance retention (b) of the Lig/PEDOT 20/80 and 60/40 in 1M $HClO_4$ electrolyte.

The Lig/PEDOT 40/60 and the prGrO film are tested in different symmetric cells and the electrochemical results are shown in Figure S6. Figure S6 a-b, show the rate performance of the symmetric cells. As expected from the 3-electrode measurements, the symmetric prGrO exhibits a higher capacitance (130 F g^{-1} per electrode, 32.5 F g^{-1} per cell) than the symmetric Lig/PEDOT 40/60 (44 F g^{-1} per electrode; 11 F g^{-1} per cell). Nevertheless, symmetric Lig/PEDOT maintains 77% of its capacitance at 10 A g^{-1}, while symmetric prGrO only retains 15 % at 3 A g^{-1}. This might be due to the balance between Lignin and PEDOT that provides an optimum charge transport. It has been reported that Lig/PEDOT's electron conductivity proceeds from tunneling between small conducting grains separated by insulating barriers[5] while prGrO has a lower conductivity given that its caused by delocalization of the electrons.[6]

Figure S6. Rate capability (a) and capacitance retention (b) of the prGrO and Lig/PEDOT 40/60 in 1 M HClO$_4$. Cyclic Voltammetry in a symmetric cell configuration at 5 mV.s-1 of Lig/PEDOT 40/60 (c) and prGrO (d). All capacitance values are reported per electrode. P.E. and N.E. denote the positive and negative electrode, respectively.

Figure S7 shows the specific energy vs power plot calculated for the composite symmetric device compared to state of the art of conductive polymers used as electrodes in symmetric cells.[7,8] Our symmetric Lig/PEDOT//prGrO device achieves similar specific energy and power values to other PEDOT cells previously reported at 5 A g^{-1}.
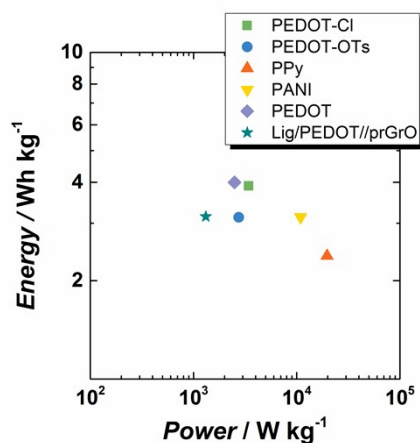
Figure S7. Ragone plot of symmetric cells using Lig/PEDOT//prGrO, Chloride- and tosylate-doped PEDOT (PEDOT-Cl and PEDOT-OTs, respectively)[7], polypyrrole (PPy), polyaniline (PANI) or PEDOT[8] as electrodes.

References

[1]   F. N. Ajjan, N. Casado, T. Rębiś, A. Elfwing, N. Solin, D. Mecerreyes, O. Inganäs, *J. Mater. Chem. A* **2016**, *4*, 1838–1847.

[2]   H.-J. Shin, S. S. Jeon, S. S. Im, *Synth. Met.* **2011**, *161*, 1284–1288.

[3]   E.-Y. Choi, T. H. Han, J. Hong, J. E. Kim, S. H. Lee, H. W. Kim, S. O. Kim, *J. Mater. Chem.* **2010**, *20*, 1907–1912.

[4]   G. Milczarek, O. Inganas, *Sci. Mag.* **2012**, *335*, 1468–1471.

[5]   S. C. Tjong, Y. W. Mai, *Physical Properties and Applications of Polymer Nanocomposites*, Woodhead Pub, **2010**.

[6]   E. H. Hwang, S. Adam, S. Das Sarma, *Phys. Rev. Lett.* **2007**, *98*, 186806–186811.

[7]   C. Karlsson, J. Nicholas, D. Evans, M. Forsyth, M. Strømme, M. Sjödin, P. C. Howlett, C. Pozo-Gonzalo, *ChemSusChem* **2016**, *9*, 2112–2121.

[8]   L. Nyholm, G. Nyström, A. Mihranyan, M. Strømme, *Adv. Mater.* **2011**, *23*, 3751–3769.